Stochastic synchronization in blinking networks of chaotic maps

Maurizio Porfiri

Phys. Rev. E **85**, 056114 — Published 17 May 2012

DOI: 10.1103/PhysRevE.85.056114

Stochastic synchronization in blinking networks of chaotic maps

Maurizio Porfiri[1, *]

[1] *Department of Mechanical and Aerospace Engineering, Polytechnic Institute of New York University Brooklyn, NY, 11201 USA*

In this paper, we analyze stochastic synchronization of coupled chaotic maps over blinking networks composed of a pristine static network and stochastic on-off couplings between any pair of nodes. We focus on mean square stability of the synchronized state by analyzing the time evolution of the second moment of the variation transverse to the synchronization manifold. By projecting the variational equations on the eigenvectors of a higher order state matrix describing this variational dynamics, we establish a necessary and sufficient condition for stochastic synchronization based on the largest Lyapunov exponent of the map and the spectral radius of such matrix. This condition is further simplified by computing closed-form results for the spectral properties of the moments of the graph Laplacian associated to the intermittent coupling and using classical eigenvalue bounds. We illustrate the main results through simulations on synchronization of chaotic Henon maps.

PACS numbers: 05.45.Gg 05.45.Pq, 05.45.Xt, 89.75.-k,

I. INTRODUCTION

Synchronization is an ubiquitous phenomenon in both natural and technological settings that has been the subject of significant research efforts in a variety of disciplines. Synchronization has been observed in a large range of phenomena spanning from biological systems, that include animal grouping [1], fireflies' blinking [2], animal gaits [3], heart stimulation [4], epidemiology [5], and neural activity [6], to secure communications [7], chemistry [8], meteorology [9], and optoelectronics [10].

Notwithstanding the vast technical literature on synchronization, the great majority of research efforts has been focused on dynamical systems that are coupled via static networks whose topology and coupling strengths do not vary in time, see for example the excellent reviews [11–15].

Here, we consider the synchronization of N maps whose individual dynamics is governed by $\mathbf{x}(k+1) = \mathbf{F}(\mathbf{x}(k))$ where $\mathbf{x} \in \mathbb{R}^m$ is the oscillator state, $\mathbf{F} : \mathbb{R}^m \to \mathbb{R}^m$ is a nonlinear function describing the system dynamics, and $k \in \mathbb{N}$ is the time variable. The oscillators are coupled through a stochastically switching network described at time k by the graph Laplacian $L(k) = [L_{ij}(k)] \in \mathbb{R}^{N\times N}$ with $i, j = 1, \ldots, N$. The equations of motion read

$$\mathbf{x}_i(k+1) = \mathbf{F}(\mathbf{x}_i(k)) - \varepsilon \sum_{j=1}^{N} L_{ij}(k)\mathbf{F}(\mathbf{x}_j(k)) \qquad (1)$$

where $i = 1, \ldots, N$ and $\varepsilon \in \mathbb{R}^+$ is the coupling strength. Here, we focus on chaos synchronization, yet, the proposed methodology is directly applicable to synchronization of nonlinear systems about fixed points or periodic orbits as well as to the analysis of coupled time-invariant linear systems, including classical consensus problems. For example, the simplest instance of this model is the case $m = 1$ and $\mathbf{F}$ equal the identity; in this case, the problem reduces to a classical consensus problem [16–18].

Synchronization of chaotic oscillators over time-varying networks finds relevant applications in modeling complex systems and engineering adaptive networks [19]; yet, only recently considerable research efforts have been devoted to this emerging field. Specifically, chaos synchronization over time-varying deterministic network topologies is considered in [20–27], while stochastic networks are examined in [28–34]. These efforts have greatly contributed to improving our understanding of chaos synchronization over time-varying networks by establishing a set of conditions for synchronization based on the node and the network dynamics.

In [35], a necessary and sufficient condition for the linear stability of the synchronized state of stochastically coupled chaotic maps is established. Such condition is based on an extension of the Master Stability Function, originally proposed in [36] for static networks, to stochastically switching weighted directed networks describing so-called conspecific agents [37]. In this network model, the cardinality of an agent's neighbor set and the weights assigned to its neighbors are given by two jointly distributed random variables and the neighbors of an agent are selected with equal probability. The fact that each oscillator is virtually not able to distinguish among others is the reason for the name "conspecific agents". While being restricted to a specific class of network models, the analysis allows to establish strong algebraic conditions similar to necessary and sufficient conditions available in the literature on consensus over stochastically switching networks, see for example in [38–42].

In this paper, we seek to extend the methodological approach proposed in [35] to blinking networks consisting of an undirected and unweighted pristine static network whose graph Laplacian is termed L_0 and stochastic on-off couplings between any pair of nodes. Such intermittent couplings have probability p to be switched on at any instant in time and they are independent of each

* mporfiri@poly.edu

other. Therefore, the matrices $L(k)$'s are independent and identically distributed matrices with common random variable $L = L_0 + \mathcal{L}$, where the random matrix $\mathcal{L}$, defining the intermittent coupling, can be regarded as the graph Laplacian of an Erdős-Rényi [43] network. We assume that switching takes place at every instant in time differently than [32], where synchronization of a lattice of logistic maps whose couplings are rewired at varying frequencies is studied.

The blinking model was originally introduced in [28] for a pristine network consisting of a regular lattice of cells with constant $2K$-nearest neighbor couplings. As discussed in [28], this model is representative of an ample class of networked natural and technological systems, including neuronal networks, packet switched networks, and pulse modulated power converters, whose sporadic interactions among the nodes regulate the overall dynamics. Therein, sufficient conditions for global chaos synchronization in a continuous-time setting are proposed based on Lyapunov stability theory. Here, we take a different approach as we focus on linear stability of the synchronization manifold and we seek to establish tractable necessary and sufficient conditions in a discrete-time setting. Notably, a similar network model is used in [40] to study stochastic link failure in consensus problems by considering a uniform intermittent coupling that is effective only on links of the pristine network. We find that our approach provides tractable sharp estimates of the convergence rate beyond the approach based on perturbation analysis proposed in [40] that is valid for p very small.

The paper is organized as follows. In Section II, we establish decoupled variational equations for the stochastic stability of the synchronization manifold. In Section III, we compute the moments of the graph Laplacian describing the blinking network. Therein, we also establish closed form results for the spectral properties of the moments of the graph Laplacian of the intermittent coupling. In Section IV, we present the main findings of this work, that is, a toolbox of mathematically tractable necessary and sufficient conditions for stochastic synchronization. In Section V, we present numerical results on synchronization of chaotic Henon maps to validate the proposed conditions and ascertain the effect of the intermittent coupling on synchronization. In Section VI, we report conclusions of this study.

II. STOCHASTIC LINEAR STABILITY OF THE SYNCHRONIZATION MANIFOLD

A. Variational equations

We say that the system of oscillators is synchronized if the state vectors for all oscillators are identical. Specifically, the oscillators are synchronized if $\mathbf{x}_1(k) = \ldots = \mathbf{x}_N(k) = \mathbf{s}(k)$ for all $k \in \mathbb{N}$ and some $\mathbf{s}$ that is a solution of the individual oscillator dynamics, that is,

$$\mathbf{s}(k+1) = \mathbf{F}(\mathbf{s}(k)) \tag{2}$$

The synchronization of (1) can be studied by linearizing the equations of motion in the neighborhood of the common trajectory $\mathbf{s}(k)$ to obtain the following variational equation

$$\boldsymbol{\xi}_i(k+1) = D\mathbf{F}(\mathbf{s}(k))\boldsymbol{\xi}_i(k) - \varepsilon \sum_{j=1}^{N} L_{ij}(k) D\mathbf{F}(\mathbf{s}(k))\boldsymbol{\xi}_j(k) \tag{3}$$

where $i = 1, \ldots, N$, $\boldsymbol{\xi}_i = \mathbf{x}_i - \mathbf{s}$ is the variation of the ith oscillator, and $D\mathbf{F}$ is the Jacobian of the function $\mathbf{F}$. By construction, the graph Laplacian is symmetric, zero-row sum, and positive semidefinite [44].

We decompose the variation of the ith oscillator into a component along the synchronization manifold and a component transverse to the synchronization manifold, that is, we write

$$\boldsymbol{\xi}_i = \widetilde{\boldsymbol{\xi}}_i + \frac{1}{N}\sum_{j=1}^{N} \boldsymbol{\xi}_j \tag{4}$$

Note that, by definition, this implies $\sum_{j=1}^{N} \widetilde{\boldsymbol{\xi}}_j = 0$. By replacing equation (4) into (3) and introducing $\widetilde{\boldsymbol{\xi}}(k) = \left[\widetilde{\boldsymbol{\xi}}_1(k)^{\mathrm{T}}, \ldots, \widetilde{\boldsymbol{\xi}}_N(k)^{\mathrm{T}}\right]^{\mathrm{T}} \in \mathbb{R}^{mN}$ where superscript T means transposition, we find the following equation for the transverse dynamics

$$\widetilde{\boldsymbol{\xi}}(k+1) = (R \otimes D\mathbf{F}(\mathbf{s}(k)) - \varepsilon L(k) \otimes D\mathbf{F}(\mathbf{s}(k)))\widetilde{\boldsymbol{\xi}}(k) \tag{5}$$

Here, $\otimes$ is the Kronecker product and $R = I_N - \frac{1}{N}\mathbf{1}_N\mathbf{1}_N^{\mathrm{T}}$, where I_N is the identity matrix in $\mathbb{R}^{N\times N}$ and $\mathbf{1}_N \in \mathbb{R}^N$ is the vector of all ones. By construction, the matrix R is an orthogonal projection onto $(\mathrm{Span}(\mathbf{1}_N))^{\perp}$ as it is symmetric, idempotent, and $\mathrm{Ker}(R) = \mathrm{Span}(\mathbf{1}_N)$, see for example [45]. Also, note that $RL = L$ since L is symmetric and zero row-sum. Equation (5) represents a discrete-time jump linear system whose state matrix depends on time, through $\mathbf{s}(k)$, and the underlying finite-state independent identically distributed random process defining the switching network [46–49]

Replacing equation (4) into (3) also yields the variational dynamics along the synchronization manifold

$$\frac{1}{N}\sum_{j=1}^{N} \boldsymbol{\xi}_j(k+1) = D\mathbf{F}(\mathbf{s}(k))\frac{1}{N}\sum_{j=1}^{N} \boldsymbol{\xi}_j(k) \tag{6}$$

Equation (6) implies that growth and decay of perturbations on the synchronization manifold are not affected by the coupling among the maps and are measured by the Lyapunov exponents of the uncoupled chaotic maps. This is due to the fact that the graph Laplacian is symmetric; such full decoupling between the variational dynamics along the synchronization manifold and the transverse dynamics is lost for directed networks [33]. In the

following, we label the Lyapunov exponents of the uncoupled chaotic maps as $h_1, \ldots, h_m$ and we use the notation $h_{\max}$ to identify the largest Lyapunov exponent.

B. Mean square stability

To study the stochastic linear stability of the synchronization manifold, we introduce the second moment matrix $\widetilde{\Xi} : \mathbb{N} \to \mathbb{R}^{mN \times mN}$ defined by $\widetilde{\Xi}(k) = \mathbf{E}\left[\widetilde{\boldsymbol{\xi}}(k)\widetilde{\boldsymbol{\xi}}(k)^{\mathrm{T}}\right]$, where $\mathbf{E}[\cdot]$ means expectation and initial conditions for the transverse dynamics are considered as parameters. By definition, $\widetilde{\Xi}(k)$ is symmetric and positive semidefinite and its trace quantifies the lack of synchronization, that is, the expected value of $\| \widetilde{\boldsymbol{\xi}}(k) \|^2$, where $\| \cdot \|$ is the Euclidean norm.

Since the matrices $L(k)$'s in (5) are independent random variables, the time evolution of $\widetilde{\Xi}$ is given by the following recursion, see also [48],

$$\begin{aligned}\mathrm{vec}(\widetilde{\Xi}(k+1)) = (&R \otimes D\mathbf{F} \otimes R \otimes D\mathbf{F} \\ &- \varepsilon R \otimes D\mathbf{F} \otimes \mathbf{E}[L] \otimes D\mathbf{F} - \varepsilon \mathbf{E}[L] \otimes D\mathbf{F} \otimes R \otimes D\mathbf{F} \\ &+ \varepsilon^2 \mathbf{E}[L \otimes D\mathbf{F} \otimes L \otimes D\mathbf{F}])\mathrm{vec}(\widetilde{\Xi}(k)) \end{aligned} \quad (7)$$

where $\mathrm{vec}(\cdot)$ denotes vectorization and we have omitted the dependence of the Jacobian on time. Here, we have used the well-known property of the Kronecker product $(A \otimes B)\mathrm{vec}(C) = \mathrm{vec}\left(BCA^{\mathrm{T}}\right)$ with A, B, and C properly sized matrices [50]. Note that (7) is a linear time-varying system since $D\mathbf{F}$ in general depends on k through $\mathbf{s}(k)$ in (2) that defines the synchronous state.

Definition 1. We say that the coupled chaotic maps in (1) stochastically synchronize if (7) is stable and we say that they do not stochastically synchronize otherwise.

Practically, the linear stability of the synchronization manifold should only be taken as a necessary condition for synchronization of a network of coupled dynamical systems. Indeed, imposing that the synchronized state is stable with respect to local perturbations of the maps' state does not necessarily imply that the maps approach a synchronized state for arbitrary initial conditions, see for example [51]. We further remark that this notion of synchronization is based on the concept of mean square stability of stochastic systems [46–48]. Equivalencies among different types of stability for linear systems can be found for example in [47]. Finally, we comment that if the matrices $L(k)$'s were not independent and rather controlled by an underlying Markov chain, as for networks of mobile oscillators considered in [30, 34, 52], the analysis of more complex recursions than (7) would be mandated following the line of argument in [46, 47].

The linear system (7) can be written in a more manageable form by expressing the matrix $\widetilde{\Xi}$ as

$$\widetilde{\Xi}(k) = \sum_{j=1}^{N^2} \left(\mathrm{vec}^{-1}\left(\mathbf{v}_j\right)\right) \otimes \Theta_j(k) \quad (8)$$

where $\mathbf{v}_1, \ldots, \mathbf{v}_{N^2}$ are linearly independent vectors in $\mathbb{R}^{N^2}$ and $\Theta_j : \mathbb{N} \to \mathbb{R}^{m \times m}$ identifies the components of $\widetilde{\Xi}$ along $\mathbf{v}_j$ for $j = 1, \ldots, N^2$. By substituting this decomposition in (7), we find the following recursion

$$\begin{aligned}&\sum_{j=1}^{N^2} \left(\mathrm{vec}^{-1}\left(\mathbf{v}_j\right)\right) \otimes \Theta_j(k+1) = \\ &\sum_{j=1}^{N^2} \left(\mathrm{vec}^{-1}\left(H\mathbf{v}_j\right)\right) \otimes \left(\mathrm{vec}^{-1}\left(D\mathbf{F} \otimes D\mathbf{F}\mathrm{vec}\left(\Theta_j(k)\right)\right)\right)\end{aligned} \quad (9)$$

where the matrix $H \in \mathbb{R}^{N^2 \times N^2}$ is defined by

$$H = R \otimes R - \varepsilon \mathbf{E}[L] \otimes R - \varepsilon R \otimes \mathbf{E}[L] + \varepsilon^2 \mathbf{E}[L \otimes L] \quad (10)$$

We note that if switching at an arbitrary frequency is considered following [32], the matrix H in (10) should be modified to include higher order statistics of the Laplacian matrix L. Indeed, if the same coupling is used for r consecutive time steps, the variational dynamics can be cast in the form of (9) by computing $\widetilde{\boldsymbol{\xi}}(k+r)$ from $\widetilde{\boldsymbol{\xi}}(k)$ in (5) and sampling $\widetilde{\Xi}$ at the switching events.

C. Master equation

The matrix H in (10) is symmetric; thus, it is diagonalizable and its eigenvectors can be taken to form an orthogonal set, see for example [50]. By selecting $\mathbf{v}_1, \ldots, \mathbf{v}_{N^2}$ in (9) to be such eigenvectors, we find

$$\mathrm{vec}(\Theta_j(k+1)) = \lambda_j(D\mathbf{F} \otimes D\mathbf{F})\mathrm{vec}(\Theta_j(k)) \quad (11)$$

where $j = 1, \ldots, N^2$ and $\lambda_1, \ldots, \lambda_{N^2}$ are the corresponding eigenvalues of H in nondecreasing order, that is, $\lambda_1 \leq \lambda_2 \ldots \leq \lambda_{N^2}$.

Therefore, according to Definition 1, the oscillators stochastically synchronize if and only if the linear time-varying system in (11) is stable for $j = 1, \ldots, N^2$. Equation (11) can be referred to as a master equation similar to those used to study synchronization of coupled maps over static networks [53–56]. For the initial orientation of the transverse error $\mathbf{u}_0 = \mathrm{vec}(\Theta_j(0))/ \| \mathrm{vec}(\Theta_j(0)) \|$ and $j = 1, \ldots, N^2$ and $\lambda_1, \ldots, \lambda_{N^2}$, equation (11) yields

$$\begin{aligned}&\lim_{k\to\infty} \frac{1}{k} \ln\left(\frac{\| \mathrm{vec}(\Theta_j(k)) \|}{\| \mathrm{vec}(\Theta_j(0)) \|}\right) = \\ &\ln|\lambda_j| + \lim_{k\to\infty} \frac{1}{k} \ln\|(D\mathbf{F}^k(\mathbf{s}(0)) \otimes D\mathbf{F}^k(\mathbf{s}(0)))\mathbf{u}_0\|\end{aligned} \quad (12)$$

where we have defined

$$D\mathbf{F}^k(\mathbf{s}(0)) = D\mathbf{F}(\mathbf{s}(k-1))D\mathbf{F}(\mathbf{s}(k-2)) \cdots D\mathbf{F}(\mathbf{s}(0)) \quad (13)$$

By invoking the ergodicity of the chaotic dynamics and recalling that $\mathbf{u}_0$ is arbitrary, see for example [15], the

right hand side of (12) takes values in $\{\ln|\lambda_j| + h_s + h_t, s, t = 1, \dots, m\}$. Therefore, equation (11) is stable for $j = 1, \dots, N^2$ if and only if $\ln \rho(H) + 2h_{\max}$ is negative where $\rho(\cdot)$ indicates the spectral radius. Thus, we establish the following result which is applicable in general to stochastically coupled chaotic maps whose dynamics is described by (1) with $L(k)$'s independent and identically distributed random variables.

Proposition 1. *The coupled chaotic maps in* (1) *stochastically synchronize according to Definition 1 if and only if*

$$\rho(H) < \kappa \tag{14}$$

where $\kappa = \exp(-2h_{\max})$ *and* $h_{\max}$ *is the largest Lyapunov exponent for the individual map.*

In the simpler cases of synchronization about fixed points or periodic orbits, Proposition 1 is still applicable and the largest Lyapunov exponent is equivalently computed from the spectral radius of the constant Jacobian $D\mathbf{F}$, that is, $\kappa = 1/\rho(D\mathbf{F})^2$, or from Floquet exponents, see for example [57], respectively. For consensus problems, $\rho(D\mathbf{F}) = 1$ and the oscillators stochastically synchronize if and only if $\rho(H) < 1$ consistently with [38]. We also comment that Proposition 1 can be easily extended to directed networks following the line of arguments in [58, 59].

For a static network, that is, $p = 0$, $\rho(H) = \rho(R - \varepsilon L_0)^2 = \max\{(1-\varepsilon\eta_2)^2, (1-\varepsilon\eta_N)^2\}$ where $\eta_1, \dots \eta_N$ are the eigenvalues of L_0 ordered in nondecreasing order with $\eta_1 = 0$ corresponding to the eigenvector $\mathbf{1}_N$, see also [56]. Therefore, (14) reduces to the classical stability result for static networks of coupled maps [53–56], that is,

$$\frac{1-\sqrt{\kappa}}{\eta_2} < \varepsilon < \frac{1+\sqrt{\kappa}}{\eta_N} \tag{15}$$

Since the so-called algebraic connectivity η_2 is different than zero if and only if the pristine network is connected [44], condition (15) implies that connectivity is necessary for synchronization. Such requirement is removed when blinking is taken into consideration as explained in what follows. We further remark that the spectral radius of $R - \varepsilon L_0$ can be attained in correspondence to either η_2 or η_N depending on the value of epsilon. Notably, in consensus problems, ε is typically assumed to be smaller than $1/\Delta$, where Δ is the largest graph degree, to enforce that the matrix $I - \varepsilon L_0$ is nonnegative. In this case, $\rho(R - \varepsilon L_0) = (1 - \varepsilon\eta_2) \leq 1$. This can be easily shown through Gerschgorin's circles which impose that $\eta_N \leq 2\Delta$, that is, $1/\varepsilon \geq \eta_N/2$, see for example [17].

III. ANALYSIS OF THE BLINKING TOPOLOGY

Equation (14) demonstrates that stochastic synchronization of (1) is controlled by the spectral properties of the matrix H which are, in turn, determined by the expected graph Laplacian $\mathbf{E}[L]$ and its autocorrelation $\mathbf{E}[L \otimes L]$ as well as the control parameter ε. In this Section, we establish closed-form expressions for $\mathbf{E}[L]$ and $\mathbf{E}[L \otimes L]$ by following a classical counting argument and we further analyze their spectral properties. We comment that weighting the links of the blinking networks differently than those of the pristine network does not modify the present analysis, yet it would require considering a secondary control parameter that would make the analysis more elaborate. For example, negative weights can be considered to model link failure.

The expected graph Laplacian is readily computed by noticing that $\mathbf{E}[L] = L_0 + \mathbf{E}[\mathcal{L}]$, that $\mathbf{E}[\mathcal{L}_{ij}] = -p$ for $i, j = 1, \dots, N$ and $i \neq j$, and that each instance of the switching network is zero-row sum. Therefore, we have

$$\mathbf{E}[L] = L_0 + pNR \tag{16}$$

Here, NR is the graph Laplacian of a complete graph and therefore the expected network is the superposition of the pristine network and a complete graph weighted by the probability p. We further comment that the eigenvalues of $\mathbf{E}[L]$ in $(\mathrm{Span}(\mathbf{1}_N))^\perp$ are $\eta_2 + pN, \dots, \eta_N + pN$.

The computation of the matrix $\mathbf{E}[L \otimes L]$ is more involved as it requires exploring correlation between link pairs. By using $L = L_0 + \mathcal{L}$ and $\mathbf{E}[\mathcal{L}] = pNR$, we find

$$\mathbf{E}[L\otimes L] = L_0\otimes L_0 + pN(L_0\otimes R + R\otimes L_0) + \mathbf{E}[\mathcal{L}\otimes\mathcal{L}] \tag{17}$$

We remark that $\mathbf{E}[L\otimes L] \neq \mathbf{E}[L]\otimes\mathbf{E}[L]$; specifically, from (16) and (17), we have

$$\mathbf{E}[L \otimes L] - \mathbf{E}[L] \otimes \mathbf{E}[L] = \mathbf{E}[\mathcal{L} \otimes \mathcal{L}] - p^2N^2R \otimes R \tag{18}$$

Below, we compute $\mathbf{E}[\mathcal{L} \otimes \mathcal{L}]$ and analyze its spectral properties.

A. Computation of $\mathbf{E}[\mathcal{L} \otimes \mathcal{L}]$

The elements of $\mathbf{E}[\mathcal{L}\otimes\mathcal{L}]$ have the form $\mathbf{E}[\mathcal{L}_{ij}\mathcal{L}_{st}]$ with $i, j, s, t = 1, \dots, N$, as per the definition of the Kronecker product which imposes a block structure in $\mathbf{E}[\mathcal{L} \otimes \mathcal{L}]$. These elements can be partitioned into six distinct cases for index values: 1) $i = j = s = t$; 2) $i = j = s \neq t$, $i = s = t \neq j$, $i = j = t \neq s$, or $j = s = t \neq i$; 3) $i = s \neq j$ and $j = t$ or $i = t \neq j$ and $j = s$; 4) $i \neq j$ and $t \neq s$ along with any of the following $i = s$ and $j \neq t$, or $i = t$ and $j \neq s$, or $j = s$ and $i \neq t$, or $j = t$ and $i \neq s$, , or $i \neq s$ and $i \neq t$ and $j \neq s$ and $j \neq t$; 5) $i = j \neq s = t$; and 6) $i = j$, $s \neq t$, $s \neq i$, $t \neq i$ or $s = t$, $i \neq j$, $i \neq s$, and $i \neq t$. As an illustration of the block structure of these

assembled terms, $\mathbf{E}[\mathcal{L}\otimes\mathcal{L}]$ with $N=3$ is

$$\left[\begin{array}{ccc|ccc|ccc} \alpha_1 & \alpha_2 & \alpha_2 & \alpha_2 & \alpha_3 & \alpha_4 & \alpha_2 & \alpha_4 & \alpha_3 \\ \alpha_2 & \alpha_5 & \alpha_6 & \alpha_3 & \alpha_2 & \alpha_4 & \alpha_4 & \alpha_6 & \alpha_4 \\ \alpha_2 & \alpha_6 & \alpha_5 & \alpha_4 & \alpha_4 & \alpha_6 & \alpha_3 & \alpha_4 & \alpha_2 \\ \hline \alpha_2 & \alpha_3 & \alpha_4 & \alpha_5 & \alpha_2 & \alpha_6 & \alpha_6 & \alpha_4 & \alpha_4 \\ \alpha_3 & \alpha_2 & \alpha_4 & \alpha_2 & \alpha_1 & \alpha_2 & \alpha_4 & \alpha_2 & \alpha_3 \\ \alpha_4 & \alpha_4 & \alpha_6 & \alpha_6 & \alpha_2 & \alpha_5 & \alpha_4 & \alpha_3 & \alpha_2 \\ \hline \alpha_2 & \alpha_4 & \alpha_3 & \alpha_6 & \alpha_4 & \alpha_4 & \alpha_5 & \alpha_6 & \alpha_2 \\ \alpha_4 & \alpha_6 & \alpha_4 & \alpha_4 & \alpha_2 & \alpha_3 & \alpha_6 & \alpha_5 & \alpha_2 \\ \alpha_3 & \alpha_4 & \alpha_2 & \alpha_4 & \alpha_3 & \alpha_2 & \alpha_2 & \alpha_2 & \alpha_1 \end{array}\right] \tag{19}$$

Case 1) describes the second moment of the degree; Case 2) represents the joint first order moment of the node degree and the its coupling with neighbors; Case 3) is the second moment of the coupling; Case 4) is the joint moment of two distinct couplings; Case 5) refers to the joint moment of degrees of two distinct nodes; and Case 6) pertains to the joint moment of the node degree and coupling of not-neighboring nodes. We denote the values taken by elements of $\mathbf{E}[\mathcal{L}\otimes\mathcal{L}]$ for these six cases as $\alpha_1, \ldots, \alpha_6$. By direct computation, we find $\alpha_1 = (N-1)(p+p^2(N-2))$, $\alpha_2 = -p-p^2(N-2)$, $\alpha_3 = p$, $\alpha_4 = p^2$, $\alpha_5 = (N-2)^2p^2+2p^2(N-2)+p$, and $\alpha_6 = -(N-1)p^2$.

In general, the $N\times N$ diagonal blocks $\mathbf{E}[\mathcal{L}\otimes\mathcal{L}]_{ii}$ and offdiagonal blocks $\mathbf{E}[\mathcal{L}\otimes\mathcal{L}]_{ij}$ with $i\neq j$ are written as

$$\mathbf{E}[\mathcal{L}\otimes\mathcal{L}]_{ii} = p(1+(N^2-N-1)p)R + N(1-p)p(R\mathbf{e}_i)(R\mathbf{e}_i)^{\mathrm{T}} \tag{20a}$$

$$\mathbf{E}[\mathcal{L}\otimes\mathcal{L}]_{ij} = -Np^2R + (1-p)p\left(\mathbf{e}_i\mathbf{e}_j^{\mathrm{T}} + \mathbf{e}_j\mathbf{e}_i^{\mathrm{T}} - \mathbf{e}_i\mathbf{e}_i^{\mathrm{T}} - \mathbf{e}_j\mathbf{e}_j^{\mathrm{T}}\right) \tag{20b}$$

where $\mathbf{e}_i\in\mathbb{R}^N$ has all zeros except of a one at the ith entry and $i,j=1,\ldots,N$.

B. Spectral properties of $\mathbf{E}[\mathcal{L}\otimes\mathcal{L}]$

The spectrum of the matrix $\mathbf{E}[\mathcal{L}\otimes\mathcal{L}]$ can be computed by using the ansatz presented in [38] to study numerosity-constrained networks. Specifically, by using a notation consistent with [38], it can be verified that

$$\widehat{\lambda}^{(1)} = 0 \tag{21a}$$

$$\widehat{\lambda}^{(2)} = pN(pN-p+1) \tag{21b}$$

$$\widehat{\lambda}^{(3)}_{\mathrm{sym}} = 2p-2p^2+p^2N^2 \tag{21c}$$

$$\widehat{\lambda}^{(3)}_{\mathrm{skew}} = p^2N^2 \tag{21d}$$

$$\widehat{\lambda}^{(4)} = pN(pN-2p+2) \tag{21e}$$

are eigenvalues of $\mathbf{E}[\mathcal{L}\otimes\mathcal{L}]$. These eigenvalues correspond respectively to eigenvectors $\mathbf{w}=[\mathbf{w}_1^{\mathrm{T}}\ldots\mathbf{w}_N^{\mathrm{T}}]^{\mathrm{T}}$ in the eigenspaces

$$\Gamma^{(1)} = \mathrm{Ker}\,(R\otimes R) \tag{22a}$$

$$\Gamma^{(2)} = \left\{\mathbf{w}\in\mathbb{R}^{N^2} : \mathbf{w}_i = \gamma_i R\mathbf{e}_i - \frac{1}{N}\sum_{j=1}^{N}\gamma_j R\mathbf{e}_j, \text{ with } \gamma_1,\ldots,\gamma_N\in\mathbb{R} \text{ such that } \sum_{j=1}^{N}\gamma_j = 0 \text{ for } i=1,\ldots,N\right\} \tag{22b}$$

$$\Gamma^{(3)}_{\mathrm{sym}} = \Big\{\mathbf{w}\in\mathbb{R}^{N^2} : \mathbf{w}_i = \sum_{k=1}^{N}\mu_{ik}\mathbf{e}_k \text{ for } i=1,\ldots,N, \text{ with } \mu\in\mathbb{R}^{N\times N} \text{ such that } \mu=\mu^{\mathrm{T}}, \mathbf{w}_i^{\mathrm{T}}\mathbf{1}_N = 0,\ \mathbf{e}_i^{\mathrm{T}}\mathbf{w}_i = 0, \text{ for } i=1,\ldots,N\Big\} \tag{22c}$$

$$\Gamma^{(3)}_{\mathrm{skew}} = \Big\{\mathbf{w}\in\mathbb{R}^{N^2} : \mathbf{w}_i = \sum_{k=1}^{N}\mu_{ik}\mathbf{e}_k \text{ for } i=1,\ldots,N, \text{ with } \mu\in\mathbb{R}^{N\times N} \text{ such that } \mu=-\mu^{\mathrm{T}}, \mathbf{w}_i^{\mathrm{T}}\mathbf{1}_N = 0,\ \mathbf{e}_i^{\mathrm{T}}\mathbf{w}_i = 0, \text{ for } i=1,\ldots,N\Big\} \tag{22d}$$

$$\Gamma^{(4)} = \Big\{\mathbf{w}\in\mathbb{R}^{N^2} : \mathbf{w} = \gamma\mathrm{vec}(R) \text{ with } \gamma\in\mathbb{R}\Big\} \tag{22e}$$

It can be verified that all these eigenspaces are orthogonal and that their dimensions are $2N-1$, $N-1$, $N(N+1)/2-2N$, $N(N-1)/2-N+1$, and 1 respectively. These dimensions sum to equal N^2 and, therefore, the dimension of each eigenspace is equal to the multiplicity of its corresponding eigenvalue.

In addition, since $N>1$, all the eigenvalues of $\mathbf{E}[\mathcal{L}\otimes\mathcal{L}]$ in (21) are nonnegative. Moreover, they can be ordered as

$$\widehat{\lambda}^{(1)} \leq \widehat{\lambda}^{(3)}_{\mathrm{skew}} \leq \widehat{\lambda}^{(3)}_{\mathrm{sym}} \leq \widehat{\lambda}^{(2)} \leq \widehat{\lambda}^{(4)} \tag{23}$$

We comment that in this blinking network model, the matrix $\mathbf{E}[\mathcal{L}\otimes\mathcal{L}]$ can take as many as five distinct eigenvalues in contrast with numerosity-constrained network models where at most four distinct eigenvalues are possible. In that case, $\Gamma^{(1)}$, $\Gamma^{(2)}$, $\Gamma^{(3)}_{\mathrm{sym}}$, $\Gamma^{(3)}_{\mathrm{skew}}$, $\Gamma^{(4)}$ are still eigenspaces, yet $\Gamma^{(3)}_{\mathrm{sym}}$ and $\Gamma^{(3)}_{\mathrm{skew}}$ have the same eigenvalue.

IV. MAIN RESULT

Using (18), the matrix H in (10) can be conveniently decomposed in

$$H = \tilde{H} + \varepsilon^2(\mathbf{E}[\mathcal{L}\otimes\mathcal{L}] - p^2N^2R\otimes R) \tag{24}$$

where $\mathbf{E}[\mathcal{L}\otimes\mathcal{L}]$ is defined in (20) and

$$\tilde{H} = (R - \varepsilon\mathbf{E}[L]) \otimes (R - \varepsilon\mathbf{E}[L]) \tag{25}$$

with $\mathbf{E}[L]$ given by (16).

The stochastic synchronization of (1) can be studied by computing the spectral radius of H and using condition (14). Nevertheless, this approach requires the computation of the spectral radius of a nonsparse large matrix, whose dimension is $N^2 \times N^2$. Such analysis is even more costly in parametric studies where we may seek to investigate the effect of varying the coupling strength ε and the probability of connection p on the synchronizability of a prescribed pristine network. Here, we establish tractable conditions for synchronization that only require the knowledge of η_2 and η_N, as in the classical master stability function, to compute of upper and lower bounds for $\rho(H)$ in terms of simple functions of p and ε.

A. Spectral analysis of H

We indicate the spectrum of the matrix $\tilde{H}$ as $\tilde{\lambda}_1, \ldots, \tilde{\lambda}_{N^2}$ and we take such eigenvalues to be organized in nondecreasing order. By using standard properties of the Kronecker product, we have that $\tilde{\lambda}_1 = \tilde{\lambda}_2 = \ldots = \tilde{\lambda}_{2N-1} = 0$, corresponding to eigenvectors in $\Gamma^{(1)}$, and the remaining eigenvalues are in the set $\mathcal{S} = \{(1-\varepsilon(\eta_i + pN))(1-\varepsilon(\eta_j + pN)),\ \text{with } i,j = 2,\ldots,N\}$, see for example [50].

The sign of these eigenvalues varies with ε and pN. Specifically, it is easy to show that the minimum and maximum eigenvalues in $\mathcal{S}$ are

$$\min\mathcal{S} = \begin{cases} (1-\varepsilon(\eta_2+pN))^2, \text{ for } \frac{1}{\varepsilon} - pN \le \eta_2 \\ (1-\varepsilon(\eta_2+pN))(1-\varepsilon(\eta_N+pN)), \\ \quad \text{for } \eta_2 \le \frac{1}{\varepsilon} - pN \le \eta_N \\ (1-\varepsilon(\eta_N+pN))^2, \text{ for } \frac{1}{\varepsilon} - pN \ge \eta_N \end{cases} \tag{26a}$$

$$\max\mathcal{S} = \begin{cases} (1-\varepsilon(\eta_N+pN))^2, \text{ for } \frac{1}{\varepsilon} - pN \le \frac{(\eta_2+\eta_N)}{2} \\ (1-\varepsilon(\eta_2+pN))^2, \text{ for } \frac{1}{\varepsilon} - pN \ge \frac{(\eta_2+\eta_N)}{2} \end{cases} \tag{26b}$$

By comparison, it can be verified that the magnitude of the minimum eigenvalue of $\tilde{H}$ is always less than or equal to the magnitude of the maximum eigenvalue, that is,

$$\rho(\tilde{H}) = \max\mathcal{S} \tag{27}$$

The matrix H has $\Gamma^{(1)}$ as an eigenspace with the null eigenvalue, since it is in the null spaces of both $\tilde{H}$ and $\mathbf{E}[\mathcal{L}\otimes\mathcal{L}]$. Computing the remaining eigenvalues is generally difficult since $\tilde{H}$ and $\mathbf{E}[\mathcal{L}\otimes\mathcal{L}]$ do not commute, that is, the eigenspaces of $\mathbf{E}[\mathcal{L}\otimes\mathcal{L}]$ in (22) are not all eigenspaces of H. Exceptions to this general case are the complete graph and the null graph for which the H and $\mathbf{E}[\mathcal{L}\otimes\mathcal{L}]$ have the same eigenspaces and the eigenvalues of H are obtained from (21) by multiplying $\widehat{\lambda}^{(2)}$, $\widehat{\lambda}^{(3)}_{\text{sym}}$, $\widehat{\lambda}^{(3)}_{\text{skw}}$, and $\widehat{\lambda}^{(4)}$ by ε^2 and then shifting them by either $(1 - 2\varepsilon pN - 2\varepsilon N + 2\varepsilon^2 pN^2 + \varepsilon^2 N^2)$ or $(1 - 2\varepsilon pN)$ depending on whether the pristine network is a complete or null graph, respectively. We note that such closed form results for Erdős-Rényi networks extend the results of [37, 41] to undirected networks.

In the general case of an arbitrary pristine network, such closed form results may be difficult to obtain. Nevertheless, the eigenvalues of the matrix H in $\left(\Gamma^{(1)}\right)^{\perp}$ can be bounded by using Weyl's inequality in (24), see for example [50]. Specifically, by projecting H on $\left(\Gamma^{(1)}\right)^{\perp}$ and using (23), we find

$$0 \le \lambda_j - \tilde{\lambda}_j \le 2\varepsilon^2 Np(1-p) \tag{28}$$

for $j = 2N, \ldots, N^2$. Here, we have used (21) to compute the smallest and largest eigenvalue of $\mathbf{E}[\mathcal{L}\otimes\mathcal{L}] - p^2N^2R\otimes R$ in $\left(\Gamma^{(1)}\right)^{\perp}$.

The bounds in (28) imply that each eigenvalue of H pertaining to $\left(\Gamma^{(1)}\right)^{\perp}$ is larger than or equal to the corresponding eigenvalue of $\tilde{H}$ and bounded away from it by at most $2\varepsilon^2 pN(1-p)$. By recalling that the smallest eigenvalue of $\tilde{H}$ is in magnitude less than or equal to the maximum eigenvalue, see (27), we have that (28) implies the following bound for $\rho(H)$

$$\rho(\tilde{H}) \le \rho(H) \le \rho(\tilde{H}) + 2\varepsilon^2 pN(1-p) \tag{29}$$

where $\rho(\tilde{H})$ is given by (26b).

If $p = 0$, the network is static and both the upper and lower bounds in (28) coincide, the spectral properties of H are equivalent to those of the static problem. If $p \neq 0$, the blinking phenomenon modifies the spectral properties of H with respect to the eigenvalues of the static problem. Notably, for p sufficiently small, the second summand in the upper bound goes to $2\varepsilon^2 pN$. Similar analysis holds if the expected degree of the Erdős-Rényi graph is held constant, that is, $p(N-1)$, as N grows. In this case, the second summand in the upper bound still goes to $2\varepsilon^2 pN$; thus, it stays well defined and the bounding is tighter as pN decreases, which, in turn, corresponds to the expected degree in the intermittent coupling.

B. Conditions for stochastic synchronization

With reference to Proposition 1 and using the bounds in (29), we establish the following manageable conditions for synchronization.

Proposition 2. *A necessary condition for stochastic synchronization of the blinking network of coupled maps described by* (1) *is*

$$\rho(\tilde{H}) < \kappa \tag{30}$$

where $\kappa = \exp(-2h_{\max})$ *and* $h_{\max}$ *is the largest Lyapunov exponent for the individual map. In addition, a sufficient condition for stochastic synchronization is*

$$\rho(\tilde{H}) + 2\varepsilon^2 pN(1-p) < \kappa \tag{31}$$

Here, $\rho(\tilde{H})$ *is given by* (27).

We remark that (30) and (31) are applicable for every selection of ε and p beyond the limit cases of sporadic link failures considered in [40] or fast switching arguments for continuous systems developed in [28]. The implementation of these conditions requires only the knowledge of the second smallest and the largest eigenvalues, η_2 and η_N, of the graph Laplacian of the pristine network and the parameter κ similarly to the classical master stability function. In this case, both p and ε play the role of control parameters that can be tuned to enforce synchronization. The former parameter measures the effect of small-world coupling due to the blinking phenomenon and the second accounts quantifies the strength of each coupling in the network.

Condition (30) is equivalent to synchronization over a static network whose graph Laplacian is $\mathbf{E}[L]$ in (16). In other words, stochastic synchronization of coupled maps over blinking networks requires that the maps synchronize over the expected network topology. Notably, following the argument for $p = 0$ leading to (15), this is possible if and only if

$$\frac{1-\sqrt{\kappa}}{\eta_2 + pN} < \varepsilon < \frac{1+\sqrt{\kappa}}{\eta_N + pN} \tag{32}$$

If such condition is satisfied, (31) can be used to determine the range of ε and p for stochastic synchronization in terms of κ, η_2, η_N, and N. Condition (32) also shows that the presence of intermittent coupling allows for smaller coupling strengths to possibly synchronize the oscillators as first established in [28]. On the other hand, synchronization is lost for smaller values of the coupling strengths in the presence of intermittent coupling. We remark that synchronization may be possible even for disconnected networks due to the blinking phenomenon, see (32) with $\eta_2 = 0$.

We comment that this very same condition can also be obtained by using the fact that mean square stability implies stability in the mean [60]. In other words, requiring that $\tilde{\Xi}(k)$ in (7) exponentially decays to zero for any initial condition implies that $\mathbf{E}[\tilde{\xi}(k)]$ also approaches zero for any initial condition. Upon taking the expectation of (5), this forces the linear stability of the synchronized state for maps that are coupled by the expected network.

For $\varepsilon \ll 1$, both the left hand sides of (30) and (31) in Proposition 2 approach $1 - 2\varepsilon(\eta_2 + pN)$, that is, $\rho(H) \simeq 1 - 2\varepsilon(\eta_2 + pN)$. This shows that synchronization over the expected network becomes a necessary and sufficient condition for stochastic synchronization in the limit of $\varepsilon \ll 1$. In other words, for ε sufficiently small, the switching network is virtually equivalent to the expected network. This scenario is thus similar to fast switching networks in [28, 33], where the oscillator dynamics is continuous in time while the network blinks intermittently.

As ε increases, the upper and lower bounds in (29) start differing and the sufficient condition (31) may be used to estimate the critical value of ε beyond which the switching network does not inherit the synchronizability of its time-average counterpart. Unfortunately, an elegant counterpart of condition (32) for finding values of p and ε that satisfy (31) cannot be found due to the presence of $2\varepsilon^2 pN(1-p)$, yet checking the sufficient condition (31) is trivial.

For $\varepsilon \gg 1$, condition (32) shows that synchronization is eventually lost. In addition, the two bounds in (29) diverge and their relative difference, defined as the difference between the upper and lower bounds divided by the upper bound, that is, $2\varepsilon^2 pN(1-p)/\rho(\tilde{H})$, approaches $2Np(1-p)/(\eta_N + pN)^2$.

V. SIMULATIONS

We consider a pristine network consisting of a lattice of $N = 25$ nodes, for which L_0 is a circulant matrix whose first row has all zeros except the first entry, which is equal to 2, and the second and last, that equal -1. For this pristine network, we have $\eta_2 = 0.0628$ and $\eta_N = 3.98$.

A. Spectral properties

We test the sharpness of the bounds in (29) by considering $p = 0.2$. This relatively large value of p, above the percolation threshold of $1/N$ [61], is selected to maximize the contrast between the bounds and best illustrate their behavior. We explore different values of the control parameters ε to explore a broad set of parameter variations.

Figure 1 displays the behavior of the bounds in the range of ε from 0 to 0.5. As expected, the bounds are initially coincident for $\varepsilon = 0$ and they start separating as ε increases until the spectral radius of H is approximately minimized. In correspondence of such minimum, the slope of both bounds suddenly changes sign. This change is located when $1/\varepsilon - pN$ is at $(\eta_2 + \eta_N)/2$, that is, at $\varepsilon = 0.142$. As ε is increased beyond the range displayed in Figure 1, the relative distance of the bounds from the spectral radius of H is preserved. For example, for $\varepsilon = 2$, $\rho(H) = 294$, the lower bound is 288 and the upper bound is 320, and for $\varepsilon = 25$, $\rho(H) = 50900$, the lower bound is 50000 and the upper bound is 55000. This demonstrates that the bounds are tight in a broad range of variation of $\rho(H)$ across five orders of magnitude. As ε is further increased, their relative difference approaches the limit value of 0.0992 confirming that the sharpness of the bound is preserved.

For the representative case $\varepsilon = 0.13$, Figure 2 reports the eigenvalues of H along with the bounds established

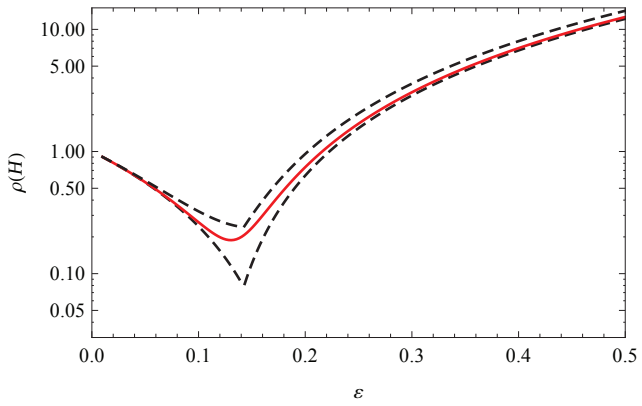

FIG. 1. (Color online) Illustration of (29) for $p = 0.2$. The red solid curve identifies $\rho(H)$ and dashed black lines the proposed sharp bounds.

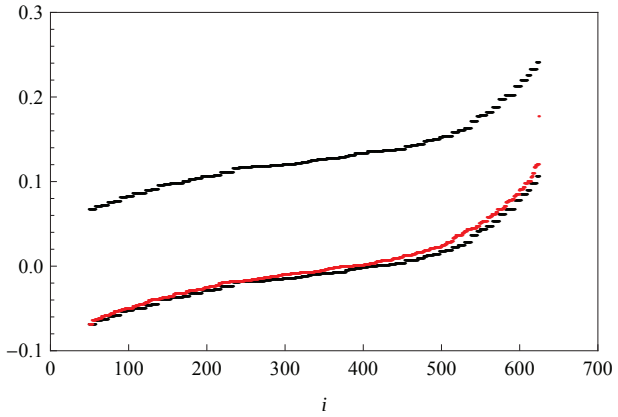

FIG. 2. (Color online) Illustration of the bounds in (28) for $p = 0.2$ and $\varepsilon = 0.13$ with eigenvalues of H in red and bounds as black dots (upper and lower data sets). Note the fact that eigenvalues can be negative and the large spectral gap between the spectral radius and the second largest eigenvalue.

in (28), demonstrating the sharpness of the proposed bounds for the whole spectrum of H.

B. Illustration of the method

We illustrate the implementation of the proposed conditions for stochastic synchronization through the analysis of canonical Henon maps coupled through the pristine network defined above. The chaotic dynamics of each individual map is governed by [35, 56]

$$x_1(k+1) = 1 - 1.4x_1^2(k) + x_2(k) \quad (33)$$
$$x_2(k+1) = 0.3x_1(k) \quad (34)$$

and its Lyapunov exponent is $h_{\max} = 0.419$ [56] so that $\kappa = \exp(-2h_{\max}) = 0.433$.

The stochastic synchronization of this system as a function of the probability of connection p and the coupling strength ε is ascertained by computing the bounds $\rho(\tilde{H}) = \max\{(1-\varepsilon(\eta_2+pN))^2, (1-\varepsilon(\eta_N+pN))^2\}$ and $\rho(\tilde{H}) + 2\varepsilon^2 pN(1-p)$ from Proposition 2. Once again, we comment that such computation requires only the knowledge of the second smallest and the largest eigenvalues of L_0. Alternatively, computing the eigenvalues of H as a function of p and ε would entail computing the spectral radius of a nonsparse matrix with dimension 625×625 for each parameter selection.

Figure 3 displays the bounds $\rho(\tilde{H})$ and $\rho(\tilde{H}) + 2\varepsilon^2 pN(1-p)$ as a function of p and ε. The region outside the yellow contour in Figure 3(a) identifies parameters' values for which synchronization is not possible according to the necessary condition in Proposition 2. On the contrary, the region within the yellow contour line in Figure 3(b) defines values of p and ε for which synchronization is possible according to the sufficient condition in Proposition 2. For $p = 0$, Figure 3(a) demonstrates that the pristine network does not support synchronization for any selection of the coupling strength. As p increases, synchronization is still not feasible for any selection of ε until p reaches approximately 0.04 as illustrated in Figure 3(a). For values of p between 0.04 and 0.09, synchronization may occur, yet the sufficient condition illustrated through Figure 3(b) does not allow to draw any conclusion. As p reaches 0.09, Figure 3(b) indicates that synchronization is possible for values of ε that are proximal to 0.2. As p further increases, Figure 3(b) shows that there is always a range of values of ε in the interval $(0, 0.2)$ for which synchronization occurs while Figure 3(a) demonstrates that synchronization is not possible as ε departs from this region by a relatively small amount of the order of 0.01.

For example, the cross-section at $p = 0.2$ can be analyzed by referring to Figure 1. Therein, by computing the intersections of each of the three curves with the horizontal line κ, we can directly extract the ranges of ε for which the maps stochastically synchronize or do not as predicted by the bounds $\rho(\tilde{H})$ and $\rho(\tilde{H}) + 2\varepsilon^2 pN(1-p)$ along with the exact range of synchronization dictated by $\rho(H)$. Specifically, we find that $\rho(H) < \kappa$ in $(0.069, 0.17)$, $\rho(\tilde{H}) < \kappa$ in $(0.068, 0.18)$, and $\rho(\tilde{H}) + 2\varepsilon^2 pN(1-p) < \kappa$ in $(0.074, 0.16)$.

As a further illustration of the proposed approach in assessing stochastic synchronization, in Figure 4, we report the evolution of the so-called error norm defined as $\delta(k) = \|(R \otimes I_m)\mathbf{x}(k)\|$, where $\mathbf{x}(k) = \left[\mathbf{x}_1(k)^{\mathrm{T}}, \ldots, \mathbf{x}_N(k)^{\mathrm{T}}\right]^{\mathrm{T}} \in \mathbb{R}^{mN}$, for $\varepsilon = 0.13$; with reference to the linear stability of the synchronization manifold presented above, this quantity equals $\| \widetilde{\boldsymbol{\xi}}(k) \|$. For this selection, $\rho(\tilde{H}) + 2\varepsilon^2 pN(1-p) = 0.188 < \kappa$, implying stochastic synchronization according to Proposition 2. We compute 40 different realizations of the blinking network and maintain the same initial conditions in the basin of attraction of the map with the two states of

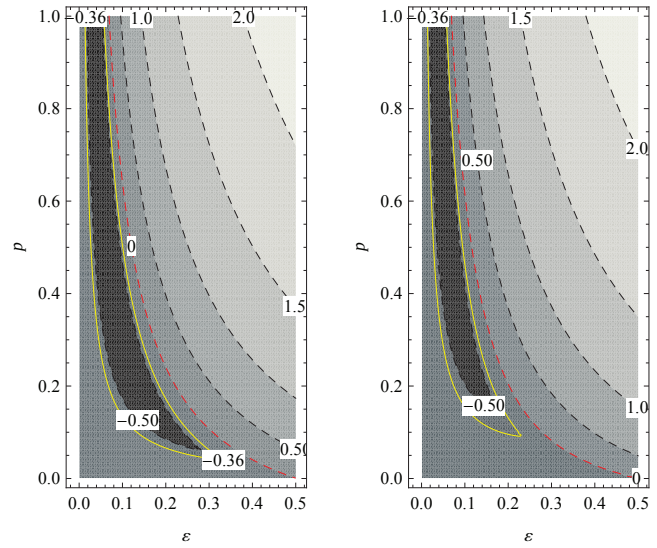

FIG. 3. (Color online) Contour plots of $\log \rho(\tilde{H})$ (a) and $\log(\rho(\tilde{H}) + 2\varepsilon^2 pN(1-p))$ (b) for $\varepsilon \in (0, 0.5)$ and $p \in (0, 1)$; logarithms are base ten. The yellow solid contour identifies $\log \kappa = -0.364$ and the red dashed line demarcates the null contour line (as made clear by the zero label superimposed).

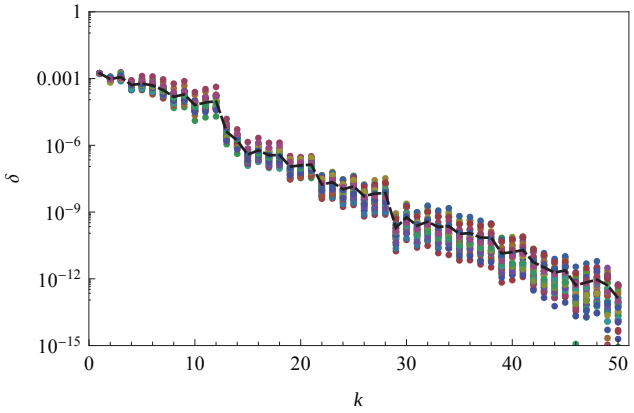

FIG. 4. (Color online) 40 time evolutions (color markers) and mean value (dashed line) of the synchronization error for $p = 0.2$ and $\varepsilon = 0.13$.

each oscillator randomly selected between 0 and 0.001. The dashed line shows the average of the numerical simulations and color markers indicate different realizations. By taking a linear regression of the average error in the logarithmic plot, we find $(2 \ln \delta(k)) \sim -0.81k$. This is in good agreement with the largest Lyapunov exponent of the error dynamics $\ln \rho(H) + 2h_{\max} = -0.83$, that is computed from Figure 1 where $\rho(H) = 0.88$.

Similarly, Figure 5 displays the evolution of the error norm for $\varepsilon = 0.06$ for which $\rho(\tilde{H}) = 0.485 > \kappa$, indicating that synchronization is not possible. In agreement with

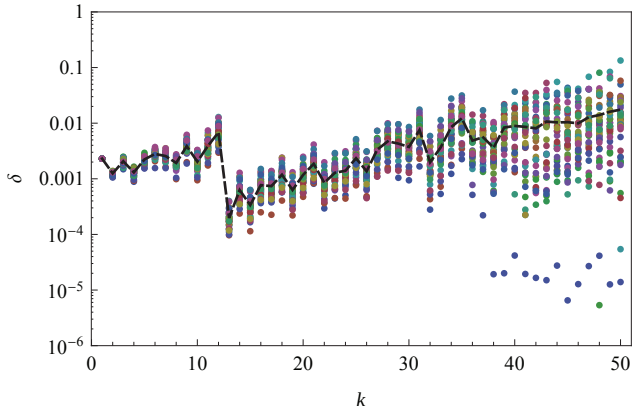

FIG. 5. (Color online) 40 time evolutions (color markers) and mean value (dashed line) of the synchronization error for $p = 0.2$ and $\varepsilon = 0.06$.

the theoretical findings, the network does not synchronize in this case; yet, the oscillators do not leave the basin of attraction and the error stays bounded.

VI. CONCLUSIONS

In this paper, we have analyzed stochastic synchronization of a network of N identical chaotic maps that are coupled by a blinking network comprised of an arbitrary static pristine graph and intermittent on-off coupling between any pair of nodes. For this network model, we have established necessary and sufficient conditions for stochastic linear stability of the synchronization manifold based on the spectral radius of a matrix of dimension $N^2 \times N^2$ and properties of an individual oscillator. Such matrix is controlled by the coupling strength ε, the probability of connection p, and the graph Laplacian of the pristine network L_0.

To cope with the computational cost associated with handling this large matrix, we have presented a toolbox of mathematically tractable necessary and sufficient conditions for synchronization based on closed-form results on the spectral properties of the intermittent coupling and classical eigenvalue bounds. These simple algebraic conditions involve only the use the second smallest and the largest eigenvalue of the graph Laplacian of the pristine network, the coupling strength, and the probability of connection. Through analytical insights and numerical simulations on Henon maps, we have demonstrated the sharpness of the proposed conditions for synchronization.

ACKNOWLEDGMENTS

This work was supported by the National Science Foundation under Grant # CMMI-0745753. The author

wishes to thank Ms. Nicole Abaid and Mr. Matteo Aureli for careful review of the manuscript.

[1] D. J. T. Sumpter, *Collective Animal Behavior* (Princeton University Press, 2009).
[2] J. Buck and E. Buck, Scientific American **234**, 74 (1976).
[3] P. L. Buono and M. Golubitsky, Journal of Mathematical Biology **42**, 291 (2001).
[4] M. R. Guevara, A. Shirier, and L. Glass, American Journal of Physiology **254**, H1 (1988).
[5] D. He and L. Stone, Proceedings of the Royal Society of London. Series B **270**, 1519 (2003).
[6] T. Womelsdorf and P. Fries, Current Opinion in Neurobiology **17**, 1 (2007).
[7] K. M. Cuomo, V. A. Oppenheim, and S. H. Strogatz, IEEE Transactions on Circuits and Systems II **40**, 626 (1993).
[8] Y. Kuramoto, *Chemical Oscillations, Waves and Turbulence* (Springer, Berlin, 1984).
[9] G. S. Duane, P. J. Webster, and J. B. Weiss, Journal of Atmospheric Sciences **56**, 4183 (1999).
[10] S. Yanchuk, A. Stefanski, T. Kapitaniak, and J. Wojewoda, Physical Review E **73**, 016209 (2006).
[11] A. Arenas, A. Diaz-Guilera, J. Kurths, Y. Moreno, and Z. Changsong, Physics Reports **469**, 93 (2008).
[12] S. Boccaletti, J. Kurths, G. Osipov, D. L. Valladares, and C. S. Zhou, Physics Reports **366**, 1 (2002).
[13] G. Chen and X. Yu, eds., *Chaos Control Theory and Applications*, Lecture Notes in Control and Information Sciences, Vol. 292 (Springer, Berlin, 2003).
[14] J. M. Gonzalez-Miranda, *Synchronization and Control of Chaos* (Imperial College Press, London, UK, 2004).
[15] A. Pikovsky, M. Rosenblum, and J. Kurths, *Synchronization, A Universal Concept in Nonlinear Sciences* (Cambridge University Press, Cambridge, 2001).
[16] W. Ren and R. Beard, *Distributed Consensus in Multivehicle Cooperative Control Theory and Applications* (Springer-Verlag, London, UK, 2008).
[17] R. Olfati-Saber, J. A. Fax, and R. M. Murray, Proceedings of the IEEE **95**, 215 (2007).
[18] D. P. Bertsekas and J. N. Tsitsiklis, *Parallel and Distributed Computation: Numerical Methods* (Athena Scientific, Belmont, MA, 1997).
[19] P. DeLellis, M. di Bernardo, T. E. Gorochowski, and G. Russo, IEEE Circuits and Systems Magazine **10**, 64 (2010).
[20] R. Amritkar and C. Hu, Chaos **16**, 015117 (2006).
[21] W. Lu, F. M. Atay, and J. Jost, SIAM Journal of Mathematical Analysis **39**, 1231 (2007).
[22] M. Chen, IEEE Transaction on Circuits and Systems I **55**, 1335 (2008).
[23] T. Liu, J. Zhao, and D. Hill, IEEE Transaction on Circuits and Systems I **57**, 2967 (2010).
[24] J. Lu, X. Yu, and G. Chen, Physica A: Statistical Mechanics and its Applications **334**, 281 (2004).
[25] D. J. Stilwell, E. M. Bollt, and D. G. Roberson, SIAM Journal on Applied Dynamical Systems **5**, 140 (2006).
[26] J. Zhao, D. J. Hill, and T. Liu, Automatica **45**, 2502 (2009).
[27] L. Wang and Q.-G. Wang, Physics Letters A **375**, 3070 (2011).
[28] I. V. Belykh, V. N. Belykh, and M. Hasler, Physica D: Nonlinear Phenomena **195**, 188 (2004).
[29] M. Frasca, A. Buscarino, A. Rizzo, L. Fortuna, and S. Boccaletti, Physical Review Letters **100**, 044102 (2008).
[30] N. Fujiwara, J. Kurths, and A. Diaz-Guilera, Physical Review E **83**, 025101(R) (2011).
[31] B. Liu, W. Lu, and T. Chen, IEEE Transactions on Automatic Control (2012).
[32] A. Mondal, S. Sinha, and J. Kurths, Physical Review E **78**, 066209 (2008).
[33] M. Porfiri, D. J. Stilwell, and E. M. Bollt, IEEE Transactions on Circuits and Systems I **55**, 3170 (2008).
[34] M. Porfiri, D. J. Stilwell, E. M. Bollt, and J. D. Skufca, Physica D **224**, 102 (2006).
[35] M. Porfiri, Europhysics Letters **96**, 40014 (2011).
[36] L. M. Pecora and T. L. Carroll, Physical Review Letters **80**, 2109 (1998).
[37] N. Abaid, I. Igel, and M. Porfiri, Linear Algebra and its Applications (2012).
[38] N. Abaid and M. Porfiri, IEEE Transactions on Automatic Control **56**, 649 (2011).
[39] T. C. Aysal, M. E. Yildiz, A. D. Sarwate, and A. Scaglione, IEEE Transactions on Signal Processing **57**, 2748 (2009).
[40] S. Patterson, B. Bamieh, and A. El Abbadi, IEEE Transactions on Automatic Control **55**, 880 (2010).
[41] S. S. Pereira and A. Pages-Zamora, IEEE Transactions on Signal Processing **58**, 2866 (2010).
[42] J. Zhou and Q. Wang, Automatica **45**, 1455 (2009).
[43] A. Erdos, P.and Renyi, Publicationes Mathematicae **6**, 290 (1959).
[44] C. Godsil and G. Royle, *Algebraic Graph Theory* (Springer-Verlag, New York, NY, 2001).
[45] G. G. Golub and C. F. Van Loan, *Matrix Computations*, 3rd ed. (Johns Hopkins, Baltimore, MD, 1996).
[46] Y. Fang and K. A. Loparo, IEEE Transactions on Automatic Control **47**, 1204 (2002).
[47] Y. Fang, *Stability analysis of linear control systems with uncertain parameters*, Ph.D. thesis, Case Western Reserve University (1994).
[48] H. J. Kushner, *Introduction to Stochastic Control* (Holt, Rinehart and Winston, Inc., New York, NY, 1971).
[49] X. Mao, *Exponential Stability of Stochastic Differential Equations* (Marcel Dekker, New York, New York, USA, 1994).
[50] D. S. Bernstein, *Matrix Mathematics* (Princeton University Press, Princeton, NJ, 2005).
[51] L. Huang, Q. Chen, Y. C. Lai, and L. M. Pecora, Physical Review E **80**, 036204 (2009).
[52] A. Buscarino, L. Fortuna, M. Frasca, and V. Latora, EPL **82**, 38002 (2008).
[53] J. Jost and M. Joy, Physical Review E **65**, 016201 (2001).
[54] W. Lu and T. Chen, Physica D: Nonlinear Phenomena **198**, 148 (2004).
[55] G. Rangarajan and M. Ding, Physics Letters A **296**, 204 (2002).
[56] A. Stefanski, J. Wojewoda, T. Kapitaniak, and

S. Yanchuk, Physical Review E **70**, 026217 (2004).
[57] J. Lu and G. Chen, IEEE Transactions on Automatic Control **50**, 841 (2005).
[58] J. Juang and Y.-H. Liang, SIAM Journal on Applied Dynamical Systems **7**, 755 (2008).
[59] T. Nishikawa and A. Motter, Physical Review E **73**, 065106(R) (2006).
[60] R. W. Brockett and J. C. Willems, "Lecture notes in mathematics, stability of stochastic dynamical systems," (1972) Chap. Average value criteria for stochastic stability, pp. 252–272.
[61] R. Durret, *Random Graph Dynamics* (Cambridge University Press, New York, NY, USA, 2007).